AD-A135 548 AN EVALUATION OF OVERLOAD RETARDATION BEHAVIOR AND OVERLOAD RETARDATION M..(U) FOREIGN TECHNOLOGY DIV WRIGHT-PATTERSON AFB OH G MINGDA ET AL. 17 NOV 83 1/1

UNCLASSIFIED FTD-ID(RS)T-1577-83 F/G 11/6 NL

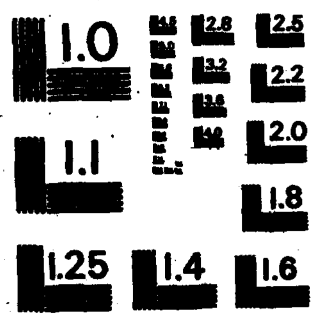
1.0
2.8
2.5
3.2
2.2
3.6
4.0
2.0
1.1
1.8
1.25
1.4
1.6

(2)

FTD-ID(RS)T-1577-83

AD-A135 548

# FOREIGN TECHNOLOGY DIVISION

AN EVALUATION OF OVERLOAD RETARDATION BEHAVIOR AND OVERLOAD RETARDATION MODELS OF Ti-6Al-4V SHEET TITANIUM ALLOY

by

G. Mingda, Z. Yongkui and Y. Minggao







83 12 09 085

# EDITED TRANSLATION

FTD-ID(RS)T-1577-83 17 November 1983

MICROFICHE NR: FTD-83-C-001394

AN EVALUATION OF OVERLOAD RETARDATION BEHAVIOR AND OVERLOAD RETARDATION MODELS OF Ti-6Al-4V SHEET TITANIUM ALLOY

By: G. Mingda, Z. Yongkui and Y. Minggao

English pages: 16

Source: Hangkong Cailiao Yanjiusuo, Vol. 1, Nr. 2, December 1981, pp. 27-34; 13

Country of origin: China
Translated by: LEO KANNER ASSOCIATES
F33657-81-D-0264
Requester: FTD/TQTA

GRAPHICS DISCLAIMER

All figures, graphics, tables, equations, etc. merged into this translation were extracted from the best quality copy available.

# An Evaluation of Overload Retardation Behavior and Overload Retardation Models of Ti-6Al-4V Sheet Titanium Alloy

Gu Mingda, Zhang Yongkui and Yan Minggao

## Abstract

This paper focuses research on overload retardation behavior under different overload ratios and different crack lengths through overload tests of a Ti-6Al-4V titanium alloy. It also discusses the effects of some major factors on retardation behavior. Retardation behavior is considered to be the result of cyclic loads. It is suggested that the retardation process can be divided into five stages. From an analysis of the modes of crack growth and other factors, the overloading process of fatigue crack growth in these tests is regarded as mainly in a plane strain condition or a mixed mode in which the plane strain occurs predominantly. Thus, at a given overload ratio $Q_{ol}$, the number of delay cycles $N_o$ caused by overload increases with the decrease of overload level $K_{ol}$ under plane strain conditions.

In this paper, the Wheeler, Willenborg, Matsuoka and Maarse models were selected in view of applications and overall comparisons and discussions were carried out regarding the describing capacity and application conditions of each model on retardation behavior. The Matsuoka model, based on the closure effect, was found to be in relatively good agreement with the test results. It was also discovered that the delay effect zones assumed in the calculation of each model were considerably smaller than the actually measured overload delay effect zones.

## I. Preface

In recent years, a great deal of attention has been given [1-3] to the prediction of fatigue crack growth life under varying loads, especially the interaction between the retardation behavior of the crack growth rate caused by overloading and the cyclic loads in the load time course. That is, the method of combining and considering the overload retardation models on the basis of the successive accumulation method in order to predict the fatigue crack growth life under varying amplitudes. Many researchers have studied the factors affecting retardation behavior from different angles. A large amount of test research has shown that retardation behavior not only depends on the overload conditions themselves but is also closely related to the fatigue failure caused by the load course before overloading. In short, retardation behavior should be the result of the interaction between the cyclic loads. It is a very complex phenomenon and to date the mechanism of retardation is still not clear. Further, the quantitative analysis of certain factors as well as their measurement is still difficult.

However, in order to explain the retardation behavior of overload and load sequence on crack growth, we successively proposed many retardation mechanisms and models and attempted to establish theoretical or empirical overload retardation models in order to provide an effective method to calculate the fatigue crack growth life under varying amplitudes in engineering.

This paper begins from the point of view of application and selects two types of models. One type is the Wheeler model [4] and Willenborg model [5] which takes the crack points having residual stress after the effects of overloading as the starting point and the other type is the Newman model [6] and Matsuoka model [7-9] which takes the crack closure effects as the starting point. The former type of model has a simple expression and its application is convenient yet it still has inadequacies. The latter type of model is relatively closer in physical concept. It is rarely used now but is being developed. For this reason, we discussed the retardation phenomena and factors for the overload tests of Ti-6Al-4V alloy sheets. We also carried out overall comparisons and evaluations of the describing capacity and application conditions etc. of the above mentioned models on the retardation phenomena.

## II. Materials and Experimental Procedure

The material used in the experiments was a Ti-6Al-4V alloy annealed sheet (thickness is 2.0mm). Its main chemical composition and mechanical properties are listed in Table 1.

| Al | V | Fe | Si | E, MPa | $\sigma_b$, MPa | $\sigma_y$, MPa | $\delta$, % | Kc, MPa$\sqrt{m}$ |
|---|---|---|---|---|---|---|---|---|
| 5.96 | 4.25 | 0.11 | <0.05 | 108000 | 1046.4 | 917.0 | 9.4 | 115.4[10] |

Table 1 Chemical composition (weight %) and mechanical properties.

The test sample is the central penetration crack type (CCT) of a longitudinal sampling. Its dimensions are 300x100x2mm and its initial crack length after prefabricated fatigue cracks is $2a_o$=20mm.

The tests were carried out on a Schenck PC 160 electrohydraulic servofatigue tester (with an SFC 16/40 computer). The stress ratio of the constant amplitude tests and the basic load cycles before and after overloading was:

[illegible]

the frequency is [illegible] [illegible] carried out at room temperature and the relative humidity was less than 60%.

See reference [11] for the explanations of the basic principles, calculation formulas and computer programs of related models.

## III. Test Results and Discussion

Constant amplitude tests were carried out according to the ASTM E647-78T. The test data was processed based on reference [12] and the processing results are listed in Table 2.

| (1) 拟合公式 | (2) 材料常数 | | | | | | | 裂纹由20mm扩展到64mm经过的载荷循环数 (3) | | |
|---|---|---|---|---|---|---|---|---|---|---|
| | $C_1$ | $m_1$ | 转折 $\Delta K_t$ (7) | $C_2$ | $m_2$ | $\varepsilon$ | VF | (4) 计算值 $N_{c,1}$ | 实测平均值 $N_e$ (5) | $\frac{N_{c,1}-N_e}{N_e}$ |
| $\frac{da}{dN}=C(\Delta K)^m$ | $5.839\times10^{-14}$ | 5.143 | 13.50 | $1.341\times10^{-7}$ | 2.515 | 0.17 | 1.33 | 103824 | 104773 | −0.91% |
| | C | | | m | | | | | | |
| $\frac{da}{dN}=\frac{C(\Delta K)^m}{(1-R)K_c-\Delta K}$ | $2.048\times10^{-6}$ | | | 2.311 | | 0.20 | 1.37 | 102920 | | −1.78% |

(6) * 表中ε为 $\frac{da}{dN}$ 拟合值与实测计算值的偏差平方和。VF为可变因子。拟合公式中，$\frac{da}{dN}$ 单位为mm/周；$\Delta K$、$K_c$单位为$MPa\sqrt{m}$。

Table. 2 Data processing results of Ti-6Al-4V sheet constant amplitude tests

Key: (1) Fitting formulas; (2) Material's constant; (3) Number of load cycles of cracks which grow from 20mm to 64mm; (4) Calculated value; (5) Average measured value; (6)* In the table, ε is the sum of partial difference squares of the $\frac{da}{dN}$ fitting value and the measured and calculated value, VF is the variable factor. In the fitting formulas, the $\frac{da}{dN}$ unit is mm/cycle; the $\Delta K$ and $K_c$ units are $MPa\sqrt{m}$; (7) Bending angle.

The a-N partial test curves under different overload ratio $Q_{ol}$ and different crack lengths are drawn in Fig. 1.

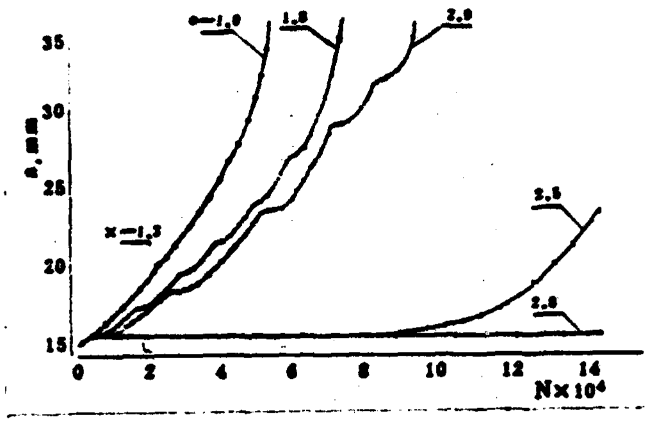


Fig. 1  a-N test curves under different $Q_{ol}$.

### 3.1  Description of Overload Models in Relation to Retardation Phenomena

In evaluating overload retardation models, we first analyze whether or not the model can appropriately describe and explain the retardation behavior as well as whether or not it grasps the major factors influencing retardation behavior. Figure 2 gives the overload retardation properties of titanium alloy when single tensile overload ratio $Q_{ol}$=2.0: da/dN-a and a-N test curve; at the same time, it gives the calculation curve corresponding to the model.

The retardation process shown on the test curve in Figure 2 is divided into five stages.

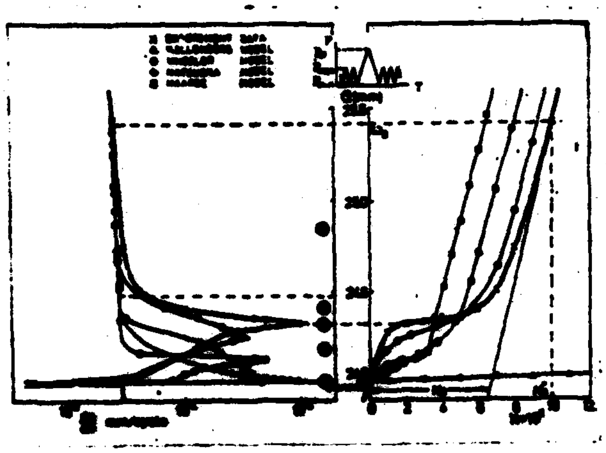

Fig. 2 Overload retardation properties of Ti-6Al-4V sheet in fatigue crack growth.

1) Crack growth acceleration stage of overload point (A) [13];
2) Hysteresis stage of overload retardation (B);
3) Maximum retardation point of overload (C);
4) Weakened stage of overload retardation (D);
5) Basic loss stage of overload retardation (E).

Note: the boundary line of stages (D) and (E) is the overload's monotone plane stress plastic zone boundary, that is

$$r_p = \frac{1}{2\pi}\left(\frac{K_{ol}}{\sigma_y}\right)^2$$

It can clearly be seen from Figure 2 that the Wheeler and Willenborg models which use the crack point's residual stress as the basis immediately reach the maximum retardation point just after overload. However, they do not show the hysteresis stage of retardation but immediately enter into the weakened stage of retardation. This explains that they are unable to describe the entire process of retardation and even more so have no way of explaining the reason for hysteresis and retardation. This is especially the case when the Willenborg model is in [illegible] calculation of the maximum retardation point of $da/dN < 10^{-9}$ mm/cycles causes the calculated life to be too large and there is already no reference value. In short, their capacity to describe retardation is quite poor. Comparatively speaking, the Matsuoka and Maarse models which use the crack closure effect as the basis can very well describe and explain the entire retardation process. Among the two, the Matsuoka model is even closer to the test curve. This explains that they grasp the crack closure and other major factors controlling retardation behavior.

It can also be seen in the figure that their maximum retardation points appeared beforehand and that the rising area crack growth rate is too short. This is the result of their omitting many retardation factors (see later discussion).

### 3.2 Comparison of Model's Estimated Value and Measured Value

Figure 3 shows the relationship between measured delay cycle number $N_0$ and overload stress strength factor $K_{ol}$ and also gives the relative values of each model calculated.

Figure 4 gives the a-N test curve under many single tensile overloads ($Q_{ol}$=1.8) as well as the entire calculation curve of each model.

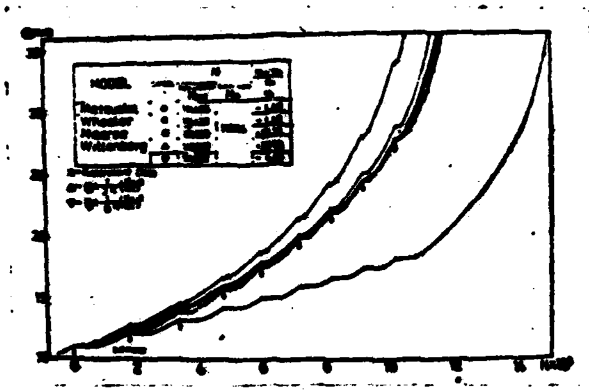

Fig. 4 a-N curve of many single tensile overloads ($Q_{ol}$=1.8).

Figure 4 also gives the measured value $N_e$ of the number of cycles required for crack growth to grow from 2a=22mm to 70mm as well as the corresponding estimated value $N_{cal}$ of the retardation model. It can be seen that not only is the Wheeler model able to regulate retardation index m(m=1.62) and obtain satisfactory results with its relative errors being -1.46% but Matsv-ka's model also obtained satisfactory results with relative errors of -1.40%. The errors of Maarse's model were -10.25%; the errors of the Willenborg model, based on the calculation of plane stress and plane strain, were separately +27.98% and -4.19%.

Figure 3 gives the $N_D$ of single tensile overload. We can see by comparing the calculation results of Figs. 3 and 4 that the errors of the estimations of single point $N_D$ are larger than those of the estimations of the entire life.

It can be seen from Figs. 1, 3 and 4 that following the increases of $Q_{ol}$, $N_D$ correspondingly has noticeable increases. This is identical to general laws [13,14] but these will not be discussed here.

Figure 3(b) does not list the calculation results of the Willenborg model because it loses effectiveness when $Q_{ol} \geqslant 2$.

These tests also measured the overload ratio without retardation of this titanium sheet under R=0.1 conditions to be 1.3 and the overload ratio without crack growth to be 2.8 (see Fig. 1). As regards this point, only Matsuoka's model was able to supply estimations and the results of estimations using this model are separately 1.40 and 2.66. Its results are still considered satisfactory.

### 3.3 Relationship of Crack Growth Mode and $N_D$

Test results prove that under given $Q_{ol}$ conditions, $N_D$ gradually decreases with the changes of $K_{ol}$ from small to large. Following this, it is basically stable or there is a slight increase (Fig. 3). This phenomenon is identical to the 2024-T3 overload test results given in reference [15].

In order to distinguish the growth mode, we carry out verification for the maximum $K_{ol}$=69MPa$\sqrt{m}$ point when $Q_{ol}$=2.0,

(1)

$$\gamma_p/B = \frac{1}{2\pi}\left(\frac{K_{ol}}{\sigma_y}\right)^2/B = 0.449 > \frac{1}{2}\ (\text{B为试样厚度}),$$

(2) $$且\ \gamma_p/a = \frac{1}{6\pi}\left(\frac{\Delta K}{2\sigma_y}\right)^2/a = 0.0021 < 0.01.$$

Key: (1) B is the thickness of the test sample; (2) And.

According to reference [16]. it should be plane strain, that is, the crack growth is the tensile mode. This can be proven from the fracture of the test sample (Fig. 5, see Plate 13): aside from the static tearing and instantaneous breaking caused by the overload itself on the fracture of the test sample, the entire crack growth surface (including the overload delay effect area) has typical plain strain fatigue fractures or only a very small part is a little sheared. Therefore, it is considered that this test belongs to the crack growth of the plane strain mode.

The influence of the crack growth mode on $M_D$ reflects the influence of overload level $K_{ol}$ on $N_D$. The dependent relationship of $N_D$ on $K_{ol}$ can be indirectly analyzed from the following formula:

$$N_D^* = \int_0^{\omega_D} \frac{da}{U_D C(\Delta K)^n}$$

In the formula, $U_D$ is the retardation coefficient. Under the given conditions of $Q_{ol}$ and R, the above formula can be roughly explained as follows: on the one hand, $N_D^*$ increases with $\Delta K$ and the assumed negative index relationship decreases sharply; on the other hand, $N_D^*$ also gradually increases with the increases of $\omega_D$. Therefore, the relationship of $N_D^*$ and $K_{ol}$ are similar as shown by the solid line in Fig. 6. When $K_{ol}$ is relatively small, it is the stress condition of the plane strain. It can be seen that under plane strain conditions, $N_D^*$ increases with the decrease of $K_{ol}$.

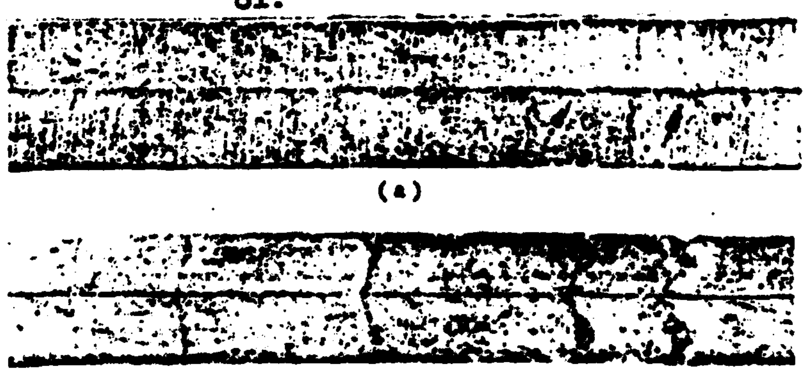

(a)

(b)

Fig. 5 (Plate 13) Front view (a) and macroscopic fracture picture (b) of test sample with single tensile overload ($Q_{ol}$=2.0) five times.

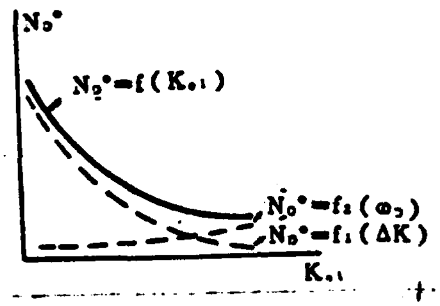


Fig. 6 Schematic diagram of the relationship between $N_D^*$ and $K_{ol}$ with given $Q_{ol}$.

Actually, under the conditions of these tests, the changes of $K_{ol}$ were in essence the changes of the crack growth. This is to say that the crack growth and crack growth type are in the same way factors which influence retardation behavior.

3.4 Relationship of $\gamma_p$, $\omega_D$ and Retardation Behavior

It is generally known that the size of overload plastic area dimension $\gamma_p$ is closely related to retardation behavior. Yet, at present, the calculation formulas used for $\gamma_p$ are only divided into the two extreme situations of plane stress and plane strain which are not sufficiently rational. On the other hand, growing fatigue cracks are still processed according to the concept of plane strain and plane stress in fracture toughness which is also not very appropriate. After a large amount of test observations, we not only consider that the growth process of fatigue cracking should primarily use plane strain but furthermore, after the discussion in the above section, we also believe that the overload process in these tests should in the same way be plane strain or a mixed mode primarily of plane strain. For this reason, using the Willenborg model listed in Fig. 4, the errors measured according to plane strain were far smaller than those calculated according to plane stress which well proves this point.

For the Matsuoka model, it was considered even more rational to introduce the cycle loading characteristics into the plastic zone of the opposite direction [16,17].

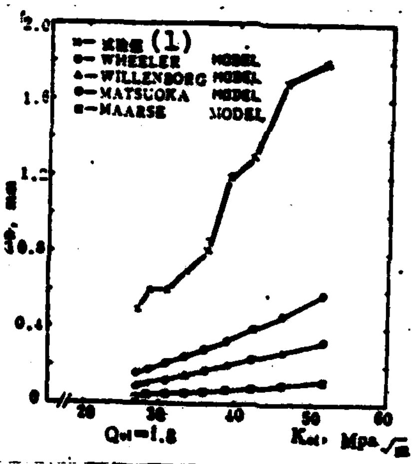


Fig. 7. Relationship of delay effect zone dimensions $\omega_D$ and $K_{ol}$.

Key: (1) Test value.

Figure 7 gives the relationship of crack growth $\omega_D$ and $K_{ol}$ which have been effected by retardation. It can be seen from Fig. 7 that $\omega_D$ correspondingly increases with the increases of $K_{ol}$. After comparisons, it can be seen that the calculation value $\omega_D$ of each model is far smaller than the measured value (about 1/2-1/15 of the measured value). Moreover, the larger $K_{ol}$ (i.e. the larger the crack length), the larger the difference value with the tests. The production of this difference value is on the one hand related to the formula of the model selected to calculate the plastic zone dimensions; on the other hand (which is an even more important reason), it is created by each model limiting the delay effect zone in the monotone plastic zone caused by a corresponding overload. Naturally, this does not accord with test results.

Test value $\omega_D$ is larger than calculated value $\omega$ of the overload's plastic zone dimensions. This also explains the control action of the crack closure effects in the retardation's basic loss stage (E). This can be explained from Fig. 2.

The five crescent moon shaped darkened crack delay growth zones are "a flight of steps" formed from the direct breaking damage of the crack tip material caused by the overload itself and the delay effect zone: after the crack edge and crack surface grow a very small distance in the 45° direction after overload, they then gradually reverse to the direction parallel to the original crack surface and continue to grow until a growth speed of a constant load is restored. It can also be seen from the figure that the width of this zone increases with the increase of the crack length and moreover the leading edge is even more protruding. In Fig. 5(a), the turning point of the crack growth direction changing and returning for the four times and five times overload effect zone is very clear.

Naturally, the protruding and restoring of the leading edge of the crack after overload, especially the turning and reversal of the crack growth direction, influence retardation behavior. However, four models do not involve this factor.

To sum up, we consider that to study retardation behavior it is not only necessary to consider the overload conditions themselves such as overload ratio, overload number etc. but it is also necessary to consider other important factors such as the closure stress (including the two sections of closure stress of the crack and crack tip which pass into and through the overload plastic zone), the crack tip's residual stress, the crack tip's passivation and sharpening, the crack tip's local strain hardening, the change and reversal of the crack tip's direction, the leading edge of the crack becoming "bow shaped" and the transformation of the crack growth mode etc. These factors are all the result of crack point surrounding plastic deformation caused by overloading. Among these, closure behavior brings about "long range" effects for each stage in the entire retardation process and thus it is presently being given serious attention.

Furthermore, the overload's environmental factors and overload's cycle stress ratio (including the negative value) are major factors affecting retardation behavior. Not all of the above mentioned models were considered and thus we must await further work.

## IV. Conclusions

1. Tests proved that the overload retardation process can be divided into five stages and that retardation behavior is the result of the interaction between cycle loads. The changes of the crack growth direction and protrusion of the leading edge of the crack can affect retardation behavior.

2. The overloading process of these tests are plane strain or mixed mode which predominantly use plane strain. Under plane strain conditions, the retardation cycle number $N_D$ correspondingly increases with the decrease of overload level $K_{ol}$ for a given $Q_{ol}$ value.

3. The results of estimating crack growth life of four retardation models with many single tensile overloads are still considered satisfactory. However, because each model limits the delay effect zone in the overload monotone plastic zone, the delay effect zone dimensions calculated for each model are much smaller than the test values.

4. The Wheeler and Willenborg models are relatively lacking in their ability to describe retardation phenomena. The expression of the former is simple and its applicability is strong yet it must measure the retardation index; the latter is simple and convenient yet loses effectiveness when $Q_{ol} \geqslant 2$.

5. The crack closure behavior plays the most important role in the entire retardation process. Thus, the ability of the Matsuoka and Maarse models with closure effects are

relatively good for describing retardation phenomena. Among them, the Matsuoka model is even closer to the test conditions. However, the effects of both of these on complex load spectrum still await further research.

A great deal of assistance was rendered by Wu Dejun, Zhang Shijie, Lu Huizhong, He Xiaohe and Ouyang Jie as well as comrades of the Room 16 Computer Group during the research process. We would like to thank them here.

## References


[1 ] "Fatigue Crack Growth Under Spectrum Loads" (original illegible) STP 595 (1976).

[2 ] Huang Yushan, Liu Xuehui and Ni Huiling, Scientific and Technical Materials of Western Engineering University, Issue 919, 1979.9.

[3 ] He Qingzhi, Journal of Beijing Aviation College, 1980, No.1.

[4 ] Wheeler, O.E., Trans. ASTM, Journal of Basic Engineering, (1972), 1, 181-186.

[5 ] Willenborg, J., Engle, R.M. and Wood, H.A., (original illegible), TM-71-1-FBR(1971).

[6 ] Maarse, J., Fracture, ICF4, 2(1977), 1025-1034.

[7 ] Matsuoka, S. and Tanaka, K., Eng. Fract. Mech. 9(1977), 507-523.

[8 ] Matsuoka, S. and Tanaka, K., Eng. Fract. Mech. 10(1978), 515-525.

[9 ] Matsuoka, S. and Tanaka, K., Eng. Fract. Mech. 11(1979), 703-715.

[10] Wanhill, R.J.H. et al., NLR TR 7404R u(original illegible) (1974).

[11] Zhang Yongkui and Gu Mingda, "Calculation Method and Program for Crack Growth Behavior," Beijing Institute of Aeronautical Materials (internal material), 1981.

[12] Zhang Yongkui and Gu Mingda, Aeronautical Materials (Special Issue), 1981, 1.

[13] Schijve, J., ASTM-STP 595 (1976), 3-23.

[14] Gu Mingda, Zhang Yongkui and Yan Minggao, Aeronautical Materials, 1979, No. 4.

[15] Crandall, G.M. and Hillberry, B.M., Fracture, ICF4, 2(1977), 1009-1015.

## References (continued)


[16] Schijve, J., Eng. Fract. Mech. 11(1979), 167-221.

[17] Jacoby, G.H. Nowack, H. and Van Lipzig, H.T.M., ASTM STP595 (1976), 171-183.


## Abstract


Overload retardation behavior under different overload ratios and different crack lengths in a Ti-6Al-4V titanium alloy has been investigated. The effect of some major factors on retardation behavior is discussed. The retardation behavior can be considered as the results of interaction effects between overload and cyclic loads. It is suggested the retardation process may be divided into five stages. From an analysis of the modes of fatigue fractures, the overloading process of fatigue crack growth in these tests can be regarded as mainly in a plane strain condition or a mixed mode in which the plane strain occurs predominantly. Thus, at a given overload ratio $Q_{ol}$ the number of delay cycles $N_D$ caused by an overload increases with a decrease of $K_{ol}$ under plane strain condition.

In this paper, the Wheeler, Willenborg, Maarse, and Matsuoka models were selected in view of engineering application. An evaluation of the describing capacity and life prediction of these models on retardation behavior have been made. The Matsuoka model based on the crack closure concept was found comparatively to be in good agreement with the experimental results. It is also recognized that the experimental values of overload delay effect zone size are considerably greater than the calculated values suggested by the above mentioned models.

ATE

LMED

8